

UniASM: Binary Code Similarity Detection without Fine-tuning

Yeming Gu¹, Hui Shu^{1,*} and Fan Hu¹

¹ State Key Laboratory of Mathematical Engineering and Advanced Computing, Zhengzhou, 450000, China

Abstract: Binary code similarity detection (BCSD) is widely used in various binary analysis tasks such as vulnerability search, malware detection, clone detection, and patch analysis. Recent studies have shown that the learning-based binary code embedding models perform better than the traditional feature-based approaches. In this paper, we proposed a novel transformer-based binary code embedding model, named UniASM, to learn representations of the binary functions. We designed two new training tasks to make the spatial distribution of the generated vectors more uniform, which can be used directly in BCSD without any fine-tuning. In addition, we proposed a new tokenization approach for binary functions, increasing the token’s semantic information while mitigating the out-of-vocabulary (OOV) problem. The experimental results show that UniASM outperforms state-of-the-art (SOTA) approaches on the evaluation dataset. We achieved the average scores of recall@1 on cross-compilers, cross-optimization-levels and cross-obfuscations are 0.72, 0.63, and 0.77, which is higher than existing SOTA baselines. In a real-world task of known vulnerability searching, UniASM outperforms all the current baselines.

Keywords: Similarity Detection; Embedding; Binary Code; NLP; Assembly Language; Vulnerability

1 Introduction

Binary code similarity detection (BCSD) is widely used in vulnerability search [1, 2], malware detection [3-5], clone detection [6, 7], patch analysis [8], etc. Most commercial software we use is only available as executable files and contains a large amount of binary code. Therefore, the study of BCSD is important for practical reasons.

One of the main challenges with BCSD is that different compilers, optimization levels, or code obfuscations can cause significant changes in the binary code. The target binaries share the same source code but lose most of the natural semantic information during the compilation process. Since the binary code does not have vocabularies with natural semantics as the source code, extracting semantic features from binary code is challenging. The existing work [9] tries to extract statistical features of instructions manually for BCSD. However, the statistical characteristics change with the compilation optimization options, resulting in a degradation of BCSD performance. Other works [10, 11] try to analyze similarity through the control flow graph (CFG). However, different compile options or code obfuscations may lead to different CFGs.

As none of the traditional similarity comparison methods have addressed the cross-optimization-levels and cross-obfuscations, the deep learning-based models are considered promising candidates for BCSD. In recent years, natural language processing (NLP) models have shown their semantic understanding and text embedding capabilities. As a result, the state-

of-the-art research in BCSD has begun to use NLP models. The Asm2vec [12], based on the PV-DM model [13], generates embeddings for instructions and functions. SAFE [14] is different from Asm2vec, and it uses the skip-gram method [15] and self-attention network [16] to generate the embeddings. However, neither PV-DM nor skip-gram can learn the complex semantic features of the binary code because they rely heavily on similar instructions in the binary code pair. Recent studies try to use more complex models: PalmTree [17] is the first to apply BERT [18] to instruction embedding, and jTrans [19] leverages BERT to learn the control flow information of the functions. They all achieved better performance than traditional methods. However, some key issues need to be studied in depth:

- Which backbone model should be chosen for binary code embedding?
- What training task is better for BCSD tasks?
- How to serialize the assembly code properly?

This paper proposes a toolkit called UniASM, which is designed for BCSD tasks and can be used directly without fine-tuning. UniASM aims to obtain high performance in BCSD tasks. We proposed a new tokenizer approach (Section 3.2) to make a balance between OOV and semantic learning. As an additional benefit, the new tokenizer makes the sequence of tokens much shorter, which can decrease the input size of the model. UniASM has designed two training tasks: Assembly Language Generation (ALG, Section 3.4.1) and Similar Function Prediction (SFP, Section 3.4.2). ALG predicts the second function in the input sequence based on unidirectional attention, while SFP predicts the similarity of the two functions in the input sequence. After training, the generated function embeddings can be used for BCSD tasks without fine-tuning.

The contributions of this paper are summarized as follows:

(1) We proposed a novel assembly language processing model, UniASM, the first UniLM-based model for BCSD. Our model outperforms the baselines and can be used in real-world BCSD tasks without fine-tuning. We have released the code and the pre-trained model of UniASM at <https://github.com/gym07/UniASM>.

(2) We proposed a new tokenizer approach for binary functions, which uses well-designed normalization of instructions to mitigate the OOV problem.

(3) We designed ablation studies to explore the impact of different backbone models, training tasks, and training corpora on the model’s accuracy in BCSD tasks. Some new findings were found that were overlooked by existing studies:

- Even without training, the UniLM-based model achieves considerable performance in BCSD tasks and is significantly better than the BERT-based model (Section 5.2.1).
- ALG task is much better than the widely used MLM task in BCSD tasks (Section 5.2.2).
- Neither random-walk nor longest-walk performs any better than the linear serialization of a function (Section 5.2.3).

2 Related works

BCSD is one of the popular research areas for binary analysis. Earlier studies tended to implement vectorization of binary codes by extracting statistical features. Solutions such as

IDA FLIRT [20] and UNSTRIP [21] identify library functions by generating fingerprints for them. DiscovRe [22] extracts statistic features to represent each basic block. Bindiff [23], Genius [24], and Kam1n0 [7] extract code features from control flow graphs and measures the binary function similarity based on graph isomorphism. Multi-MH [25], BinGo [26], and IMF-sim [27] capture behaviors of a binary function by sampling it with random values.

Graph embedding is one of the popular learning-based studies. Gemini [11] extracts attributed control flow graph (ACFG) for functions and trains a graph embedding network to generate embeddings. Order Maters [28] adopts a convolutional neural network (CNN) on adjacency matrices to extract the order information of CFG. BugGraph [10] utilizes a graph triplet-loss network on the attributed control flow graph to produce a similarity ranking.

Another learning-based study has been inspired by natural language processing (NLP). Asm2vec generates embeddings for instructions and functions by the PV-DM model. SAFE uses skip-gram to generate instruction embeddings and then utilizes a self-attentive neural network to generate function embeddings. PalmTree applies BERT to instruction embedding and shows the great potential of language models in BCSD. jTrans is the first study to embed control flow information of binary code into Transformer-based language models. INNEREYE [2] utilizes word embedding and Long Short-Term Memory (LSTM) to capture the semantics and dependencies of instructions automatically.

3 Methodology

3.1 Overview

UniASM is mainly inspired by SimBERT [29] and UniLM [30]. UniLM uses bidirectional and unidirectional attention to achieve semantic understanding and generative capabilities. SimBERT proposed a new similarity query task for each batch. UniASM is a transformer-based model and uses two training tasks: Assembly Language Generation (ALG) and Similar Function Prediction (SFP). ALG leverages unidirectional attention to generate the second half of the sequence. SFP is a function query task similar to the query task in SimBERT, which enables the generated function embeddings to be used directly in the BCSD tasks.

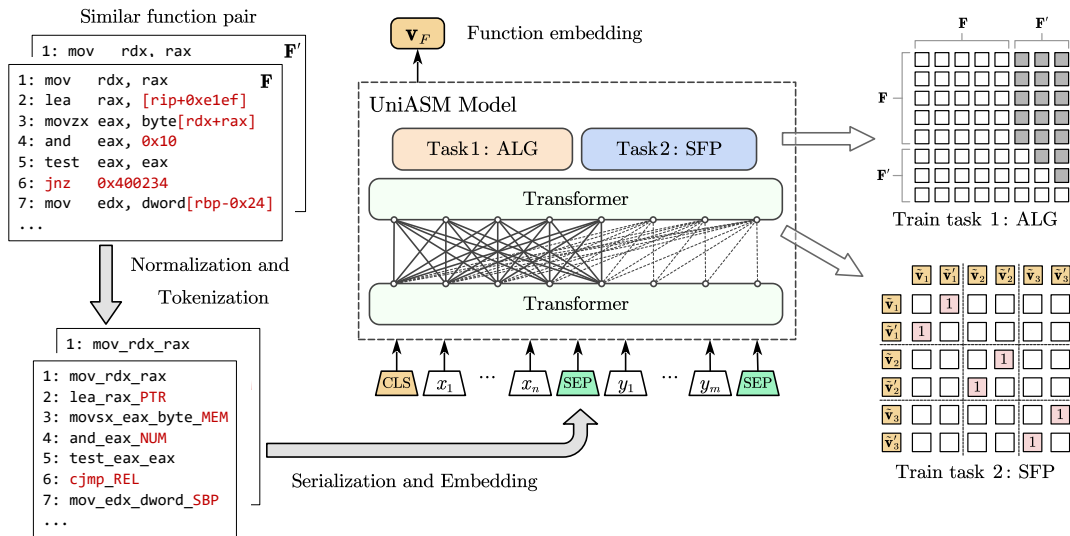


Figure 1: Overview of UniASM

Figure 1 shows the overview of UniASM. For training, the input sequence is constructed from a pair of similar functions. First, the instructions of the functions are normalized to remove the noisy words and mitigate the OOV problem. Then, the instructions are tokenized according to a simple principle: one instruction produces one token. Next, we use a simple linear serialization approach to convert a function to a sequence of tokens. Finally, the sequence is used as the input of UniASM.

For evaluation, the input sequence is constructed from one function, and the output of the model is the function embedding. We compute the cosine similarity between the two function embeddings as our model-predicted similarity.

3.2 Normalization and Tokenization

The raw representation of a binary function is a series of instructions that cannot be used directly. We designed a new representation approach for binary functions. It mainly contains three stages: instruction normalization, assembly tokenization, and function serialization.

3.2.1 Instruction normalization

Instruction normalization makes instructions look cleaner by replacing the addresses, immediate numbers, float instructions, and conditional jumps. The main principles are as follows:

- The indirect addressing with register “eip/rip” is replaced by “PTR”
- The indirect addressing with register “esp/rsp” is replaced by “SSP”
- The indirect addressing with register “ebp/rbp” is replaced by “SBP”
- Other indirect addressing is replaced by “MEM”
- The relevant addressing is replaced by “REL”
- The immediate number is replaced by “NUM”
- The float instruction with register “xmm” is replaced by “XMM”
- The conditional jump, such as “jnz,” is replaced by “cjmp”

3.2.2 Assembly tokenization

Tokenization breaks unstructured data and text into chunks of information that can be considered discrete elements called tokens. In this paper, the whole instruction is regarded as a token. The advantage is that the instruction contains richer semantic information than individual operands. In practice, we replace the white space with an underline for an instruction, e.g., “mov rax, 0x10” will be represented by the token “mov_rax_NUM.” The ablation studies (Section 5.2) show that this whole-instruction tokenization approach performs much better than the small-token approach.

3.2.3 Function serialization

Function serialization aims to serialize the structured function into a sequence of tokens. The approach used in this paper is to serialize the function directly in linear order (address order). Experimental results show that linear serialization performs similarly to random-walk and longest-walk (Section 5.2.3). However, random-walk and longest-walk require the construction of a CFG of the function, which is time-consuming. Even worse, the longest-walk has to search the longest path on the CFG, which is difficult.

3.3 Backbone network

The base model used in UniASM is a transformer model, as shown in Figure 2, which has shown a strong capability in the representation learning of natural semantics. According to the processing flow, it can be divided into three parts: the token embedding layer, the self-attention layer, and the function embedding layer.

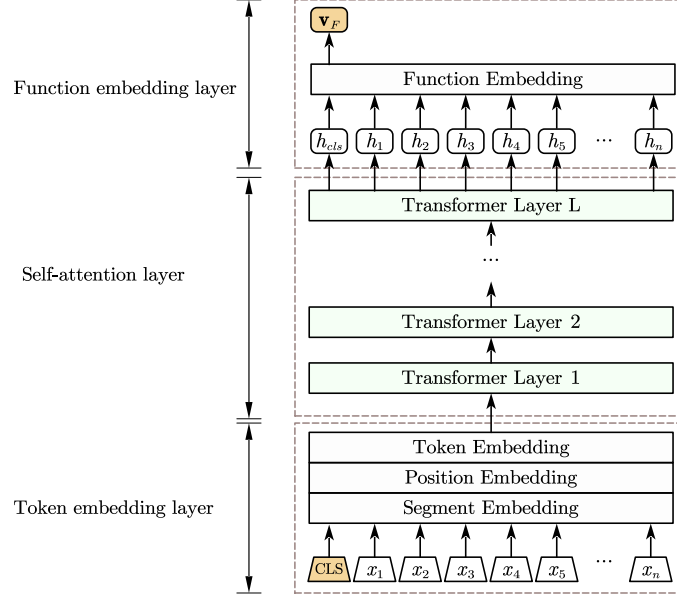


Figure 2: Backbone network

3.3.1 Token embedding layer

The token embedding layer is used to generate the input vector for the token sequence of the function. For the token sequence of the input function $\mathbf{F} = [x_1, x_2, \dots, x_n]$, where x_i represent the i -th token of the function, the input vector $\mathbf{H}^0 = [E(x_1), E(x_2), \dots, E(x_n)]$ is obtained by summing the token embedding Ex_i , position embedding Ep_i , and segment embedding Es_i : $E(x_i) = Ex_i + Ep_i + Es_i$.

3.3.2 Self-attention layer

The self-attentive layer consists of multiple transformer layers stacked on top of each other, as shown in Figure 2. The input vector $\mathbf{H}^0 = [E(x_1), E(x_2), \dots, E(x_n)]$ is used as the input to the first layer of the Transformer. For the Transformer of the total number of L layers, the output of the l -th layer is represented as $\mathbf{H}^l = \text{Transformer}_l(\mathbf{H}^{l-1})$, $l \in [1, L]$, and the self-attention is calculated as follows:

$$\mathbf{Q}_l = \mathbf{H}^{l-1} \mathbf{W}_l^Q, \mathbf{K}_l = \mathbf{H}^{l-1} \mathbf{W}_l^K, \mathbf{V}_l = \mathbf{H}^{l-1} \mathbf{W}_l^V$$

$$\mathbf{M}_{ij} = \begin{cases} 0, & \text{allow to attend} \\ -\infty, & \text{prevent from attending} \end{cases}$$

$$\mathbf{A}_l = \text{softmax} \left(\frac{\mathbf{Q}_l \mathbf{K}_l^\top}{\sqrt{d_k}} + \mathbf{M} \right) \mathbf{V}_l$$

where the output of the previous layer \mathbf{H}^{l-1} generates \mathbf{Q}_l , \mathbf{K}_l and \mathbf{V}_l through three parameter matrices \mathbf{W}_l^Q , \mathbf{W}_l^K , \mathbf{W}_l^V . The mask matrix \mathbf{M}_{ij} defines the attention between the tokens. The output \mathbf{A}_l is summed with the \mathbf{H}^{l-1} residual operation and the feedforward network finally generates a new hidden layer vector \mathbf{H}^l .

3.3.3 Function embedding layer

The function embedding layer generates the embedding vector of the input function. In this paper, we calculate the function embedding vector by the output vector of the token ‘‘CLS’’:

$$\mathbf{v}_F = \tanh(h_{\text{CLS}}) \cdot \mathbf{W}^F,$$

where $\tanh(\cdot)$ is the activation function, \mathbf{W}^F is the parameter matrix of the fully connected network.

3.4 Training tasks

UniASM abandons the commonly used mask language model (MLM) and next sentence prediction (NSP) pre-training tasks of BERT in favor of the Assembly Language Generation task (ALG, Section 3.4.1) and the Similar Function Prediction task (SFP, Section 3.4.2).

3.4.1 Assembly Language Generation

ALG leverages an attention mask matrix to define bidirectional attention and unidirectional attention. As shown in Figure 3, the first function in the input sequence uses bidirectional attention, while the second function uses unidirectional attention. It allows the model to generate the second function according to the first one.

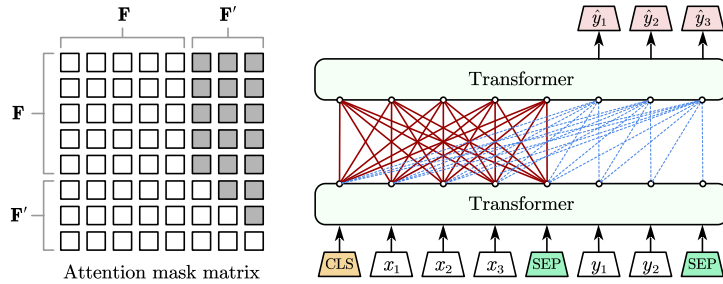


Figure 3: Assembly Language Generation

For the input pair of functions $\mathbf{F}=[x_1, x_2, \dots, x_n]$ and $\mathbf{F}'=[y_1, y_2, \dots, y_m]$, the input tokens for UniASM are $[\text{CLS}, x_1, \dots, x_n, \text{SEP}, y_1, \dots, y_m, \text{SEP}]$. The goal of ALG is to correctly predict the second function \mathbf{F}' according to the first function \mathbf{F} . When we got the predict value $\hat{\mathbf{F}}'=[\hat{y}_1, \hat{y}_2, \dots, \hat{y}_m]$, the *softmax* is applied to the result:

$$p(\hat{y}_i | \mathbf{F}) = \frac{\exp(\hat{y}_i)}{\sum_{k=1}^m \exp(\hat{y}_k)},$$

where \hat{y}_i denotes the predict value of y_i . ALG uses cross-entropy to calculate the loss as follows:

$$\min_{\theta} \mathcal{L}_{ALG}(\theta) = \sum_i -\log p(\hat{y}_i | \mathbf{F})$$

3.4.2 Similar Function Prediction

SFP processes one batch at a time rather than a pair of functions. As shown in Figure 4, each sample in the batch is a pair of similar functions, such as $[\text{CLS}] \mathbf{F} [\text{SEP}] \mathbf{F}' [\text{SEP}]$, where \mathbf{F} and \mathbf{F}' are similar functions. We swap these two functions to construct a new sample $[\text{CLS}] \mathbf{F}' [\text{SEP}] \mathbf{F} [\text{SEP}]$ and place it after the original one. So, each batch should contain an even number of samples.

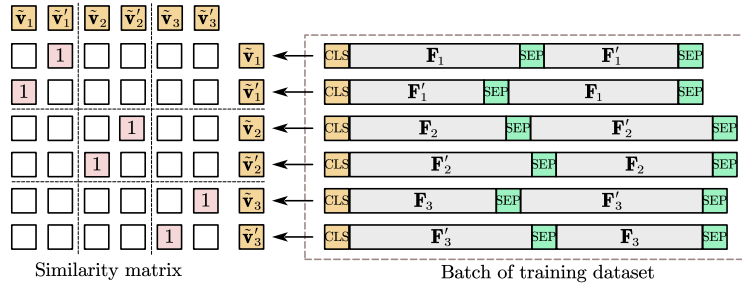


Figure 4: Similar Function Prediction

The embedding of the k -th function in the batch is $\mathbf{v}_k=[v_1, v_2, \dots, v_d]$, where d is the hidden size. Then the elements in the vector are L2 normalized:

$$\tilde{v}_i = \frac{v_i}{\sqrt{\sum_{j=1}^d v_j^2}}.$$

The normalized function embedding vector can be obtained: $\tilde{\mathbf{v}}_k = [\tilde{v}_1, \tilde{v}_2, \dots, \tilde{v}_d]$. We take all the normalized vector of the batch to construct the embedding matrix $\tilde{\mathbf{V}} = [\tilde{\mathbf{v}}_1, \tilde{\mathbf{v}}_2, \dots, \tilde{\mathbf{v}}_b]^\top$, where b is the batch size.

To calculate the similarity between two functions in the batch, we dot product the embedding matrix $\tilde{\mathbf{V}}$ with its transpose matrix $\tilde{\mathbf{V}}^\top$:

$$\mathbf{S} = \tilde{\mathbf{V}} \cdot \tilde{\mathbf{V}}^\top = \{s_{ij}\}, i, j \in [1, 2, \dots, b].$$

The result \mathbf{S} is called the similarity matrix. Each value in the similarity matrix denotes the similarity of two functions. The idea is based on the fact that the value of the dot product of unit vectors is equal to $\cos(\varphi)$, where φ denotes the angle between two vectors. The more similar the vectors are, the smaller the angle between them should be. That is, the dot product of vectors of similar functions should be closer to 1, and the dot product of vectors of different functions should be closer to -1.

It should be noted that values on the diagonal in the similarity matrix are all equal to 1 because they are dot products of the same unit vector. However, what we really care about is the value of the two similarity functions. To avoid the effect of the diagonal elements, we set all diagonal elements to negative infinity:

$$\mathbf{S} = \tilde{\mathbf{V}} \cdot \tilde{\mathbf{V}}^\top - \Lambda[+\infty],$$

where $\Lambda[+\infty]$ denotes a diagonal matrix, whose values are infinity. For each row in the matrix, it needs to be processed by *softmax* layer as:

$$p(s_{ij}) = \frac{\exp(s_{ij})}{\sum_{k=1}^b \exp(s_{ik})},$$

where s_{ij} denotes the similarity of the i -th function and the j -th function in the batch. SFP uses cross-entropy to calculate the loss as follows:

$$\min_{\theta} \mathcal{L}_{SFP}(\theta) = \sum_k -\log p(s_{ik}).$$

The loss function of UniASM is the combination of the two loss functions:

$$\min_{\theta} \mathcal{L}(\theta) = \mathcal{L}_{ALG}(\theta) + \mathcal{L}_{SFP}(\theta).$$

4 Experimental setups

4.1 Dataset

4.1.1 Training dataset

As shown in Table 1, we collected seven open-source projects commonly used under Linux as the training dataset for UniASM.

Table 1: Projects used for training

| Datasets | Version | Binaries | Functions (GCC-O0) | ASM files |
|-----------|---------|----------|--------------------|-----------|
| Binutils | 2.37 | 16 | 5,465 | 107,098 |
| Coreutils | 9.0 | 106 | 2,321 | 47,406 |
| Diffutils | 3.8 | 4 | 592 | 12,008 |
| Findutils | 4.8.0 | 4 | 898 | 18,135 |
| Tcpdump | 4.9.3 | 1 | 1,448 | 32,243 |
| Gmp | 6.2.1 | 1 | 760 | 16,777 |
| Curl | 7.82.0 | 1 | 1,210 | 26,455 |
| Total | - | 133 | 12,694 | 260,122 |

Compilation We used different compilers (GCC-7.5, Clang-10) with four optimization levels (O0, O1, O2, O3). In addition, the obfuscator (Ollvm14) [31, 32] is used to generate different obfuscated codes (*-sub*, *-fla*, *-bcf*) with the four optimization levels, where *-sub* denotes instruction substitution, *-fla* denotes control flow flattening, *-bcf* denotes bogus control flow. Thus, we can get 11 different results for each of the input functions. It should be noted that all source codes are compiled with the option *-fno-inline* to avoid function inlining. The main reason is that the function inlining can interfere with similar function pairs, which is detrimental to the training of the model. After the compilation, a total of 1596 binaries were obtained.

Disassembly UniASM is designed to generate embeddings for assembly codes. We did the disassembly with the help of Radare2 [33] and saved the functions in separate files. There is a slight difference in the number of functions obtained by disassembling the binary for different compilation options and code obfuscations. We got 12,694 unique functions (GCC O0) and about 260K disassembly files.

Similar function pairs The training data for UniASM are similar function pairs. As shown in Table 2, we combine some of the different disassembly results for each function to form 40 similar function pairs. The numbers in the table indicate the number of function pairs to be generated, “-” means no function pairs are generated. For the same compiler, only the optimization level needs to be considered, and there are six combinations (O0/O1, O0/O2, O0/O3, O1/O2, O1/O3, and O2/O3). For the different compilers, all 16 combinations are considered. For the code obfuscations, we only combine the obfuscated code with the normal code because we expect UniASM to learn the obfuscation features. We obtained about 500K similar function pairs in total.

Table 2: Function pairs generated

| | GCC7.5 | Clang10 | Ollvm14-sub | Ollvm14-fla | Ollvm14-bcf |
|---------|--------|---------|-------------|-------------|-------------|
| GCC7.5 | 6 | 16 | - | - | - |
| Clang10 | - | 6 | - | - | - |
| Ollvm14 | - | - | 4 | 4 | 4 |

Dataset generation We generate two sequences for each function pair. First, small functions with less than ten instructions are filtered to avoid semantically meaningless functions. Then, we generate a new function pair by swapping the two functions. Next, the tokenizer converted each function pair to a token sequence. Finally, we shuffle all the sequences randomly and divide them into two parts: 90% for training and 10% for validation. The training dataset contains 428K sequences, and the validation dataset contains about 47K sequences.

4.1.2 Evaluation dataset

This paper prepared a test dataset to evaluate our model and the baselines. The dataset is generated by the open-source project libpcap-1.9.1, which is not included in the training dataset. The same software may have coding habits, functional characteristics, compilation environment, and other factors that may lead to information leakage in the test set, resulting in experimental result preference. Therefore, this paper uses binary programs that the training process has not seen as a test set to make the results more general.

The projects were compiled by different compilers (GCC, Clang) with the four optimization levels (O0, O1, O2, O3) and by Ollvm14 with three obfuscations (-sub, -fla, -bcf). The number of functions for each compilation environment varies from 314 (Clang-O3) to 531 (Ollvm-bcf).

4.2 Baselines

We compare UniASM to the following four baselines:

Asm2vec [12] is a PV-DM-based model for assembly language embedding. It uses random walks on the CFG to sample instruction sequences and then uses the PV-DM model to learn the embedding of the assembly language. The original paper of Asm2vec shows that their dataset contains function names of system libraries, but our validation dataset does not contain this kind of information. Asm2vec is not open source, we used an unofficial version [34] that is publicly available. We used the default parameters for evaluation.

SAFE [14] is an Attention-based model for assembly language embedding. It employs an RNN architecture with attention mechanisms to generate function embeddings. We used their official open-source code and pre-trained model [35] for evaluation, with its default parameters.

PalmTree [17] is a BERT-based model for assembly instruction embedding. It uses three pre-training tasks to learn the characteristics of assembly instructions and generates the instruction embeddings. We implemented this baseline based on their official open-source code and pre-trained model [36] with its default parameters.

jTrans [19] is a jump-aware BERT-based model for assembly language embedding. It retains the jump relationships between instructions when generating input samples for BERT, allowing BERT to learn the control flow information of the code. We used their official open-source code and pre-trained model [37] for evaluation, with its default parameters.

4.3 Evaluation Metrics

The task of function similarity search is often used to measure the performance of BCSD models. The function similarity search aims to find similar functions in a large pool of functions for the input function. The input function is selected from a source function pool, and the model searches the target function pool to find similar functions. The source and target function pools are defined as:

$$\mathcal{F}_{src} = \{f_1, f_2, \dots, f_i, \dots, f_n\}$$
$$\mathcal{G}_{dst} = \{g_{f_1}, g_{f_2}, \dots, g_{f_i}, \dots, g_{f_n}\}.$$

The source function pool \mathcal{F}_{src} contains n functions, i.e., the pool size is n . Each input function $f_i \in \mathcal{F}_{src}$ corresponds to a ground truth function $g_{f_i} \in \mathcal{G}_{dst}$.

The metrics of Mean Reciprocal Rank (MRR) and Recall@k are used to evaluate the performance. We take the top- k results for each query and sort them according to the similarity score. The MRR metric is the average of the reciprocal ranks of results for a sample of the queries, while the Recall@ k metric is the ratio of successful queries to the pool size (a successful query means the true ground function is in the top- k results):

$$\text{MRR}(\mathcal{F}_{src}) = \frac{1}{|\mathcal{F}_{src}|} \sum_{f_i \in \mathcal{F}_{src}} \frac{1}{\text{Rank}(g_{f_i} | f_i)}$$

$$\text{Recall}@k(\mathcal{F}_{src}) = \frac{1}{|\mathcal{F}_{src}|} \sum_{f_i \in \mathcal{F}_{src}} \mathbb{I}[\text{Rank}(g_{f_i} | f_i) \leq k],$$

where $\text{Rank}(g_{f_i} | f_i)$ refers to the rank position of the first hit function for the i -th query. •

\mathbb{I} is an identity function that outputs 1 if the expression inside is evaluated to be true and 0 otherwise.

4.4 Hyperparameter Selection

We chose the following hyperparameters for UniASM: 4 transformer layers, 12 attention heads, embedding size of 256, vocabulary size of 21000, and intermediate size of 3072. For training, we chose the batch size of 8, and the learning rate is set to 5e-5 with the warmup of 4 steps.

5 Evaluation

The evaluation aims to answer the following questions:

RQ1: How accurate is UniASM in BCSD tasks compared with other baselines? (Section 5.1)

RQ2: What impact do different backbone models, training tasks, and training corpora have on the model’s accuracy in BCSD tasks? (Section 5.2)

RQ3: How effective is UniASM at searching known vulnerabilities? (Section 5.3)

All programs are compiled and pre-processed on an Ubuntu 20.04 server with 16GB RAM and Intel 8 core 3.0GHz CPU. In most cases, we use Radare2 for disassembling binary programs to generate assembly code. One of the baseline methods, jTrans, requires IDA pro [38] to disassemble the binary program. We trained UniASM on one TPU v3-8 chip, and all evaluation experiments were run on our laptop with Intel Core i7-9750H CPU, 32GB RAM, and NVIDIA GeForce GTX 1650 4GB GPU.

5.1 Performance

This paper evaluated UniASM and the baselines on three BCSD tasks: cross-compilers (GCC-7.5/Clang-10), cross-optimization-levels (GCC-7.5, O0/O1/O2/O3) and cross-obfuscations (Ollvm14, sub/fla/bcf). Table 3-5 shows the scores of MRR and Recall@1 for

UniASM and the baselines. The Recall@1 metric captures the ratio of functions correctly matched at the first position of the search results.

5.1.1 Cross Compilers (X-COM)

In this evaluation, we generated function pools for each optimization level. The function pools of GCC were used as the source pools of searching, while the pools of Clang were used as the target pools. As shown in Table 3, there are four searching tasks: “O0” is short for “GCC-O0 vs. Clang-O0,” “O1” is short for “GCC-O1 vs. Clang-O1,” etc. UniASM achieved average MRR and Recall@1 values of 78% and 72%. It outperforms its closest baseline competitor by 28% and 44%.

Table 3: Performance on cross-compilers (X-COM)

| | MRR (GCC vs. Clang) | | | | | Recall@1 (GCC vs. Clang) | | | | |
|----------|---------------------|------------|------------|------------|------------|--------------------------|------------|------------|------------|------------|
| | O0 | O1 | O2 | O3 | Avg. | O0 | O1 | O2 | O3 | Avg. |
| Asm2vec | .42 | .51 | .42 | .45 | .45 | .30 | .43 | .35 | .37 | .36 |
| SAFE | .72 | .67 | .50 | .56 | .61 | .59 | .56 | .40 | .45 | .50 |
| PalmTree | .31 | .45 | .42 | .47 | .41 | .20 | .36 | .34 | .38 | .32 |
| jTrans | .55 | .55 | .55 | .57 | .55 | .43 | .41 | .41 | .43 | .42 |
| UniASM | .92 | .82 | .66 | .71 | .78 | .87 | .76 | .60 | .64 | .72 |

5.1.2 Cross Optimization levels (X-OPT)

In this evaluation, the function pool of optimization level “O0” was used as the source pool of searching, and the pools of other optimization levels were used as the target pools. We have done this evaluation for GCC and Clang, respectively. As shown in Table 4, “O0,O1” is short for “GCC-O0 vs. GCC-O1/Clang-O0 vs. Clang-O1,” “O0,O2” is short for “GCC-O0 vs. GCC-O2/Clang-O0 vs. Clang-O2,” etc. The left of the two scores in the cell is for GCC, and the right is for Clang. UniASM outperforms all the baseline models by considerable margins. In the most challenging task, “Clang-O0 vs. Clang-O2,” UniASM still achieved MRR and Recall@1 values of 57% and 50%, while the closest baseline achieved 39% and 27%.

Table 4: Performance on cross-optimization-levels (X-OPT)

| | MRR (GCC/Clang) | | | | Recall@1 (GCC/Clang) | | | |
|----------|-----------------|----------------|----------------|----------------|----------------------|----------------|----------------|----------------|
| | O0,O1 | O0,O2 | O0,O3 | Avg. | O0,O1 | O0,O2 | O0,O3 | Avg. |
| Asm2vec | .24/.13 | .20/.12 | .19/.13 | .21/.13 | .16/.08 | .13/.06 | .12/.07 | .14/.07 |
| SAFE | .50/.50 | .44/.36 | .38/.37 | .44/.41 | .36/.35 | .31/.26 | .27/.27 | .31/.29 |
| PalmTree | .12/.07 | .09/.06 | .09/.07 | .10/.06 | .07/.04 | .05/.04 | .06/.05 | .06/.04 |
| jTrans | .57/.46 | .56/.39 | .53/.41 | .55/.42 | .43/.33 | .41/.27 | .39/.29 | .41/.30 |
| UniASM | .81/.81 | .76/.57 | .63/.61 | .73/.66 | .73/.74 | .69/.50 | .57/.53 | .66/.59 |

5.1.3 Cross Obfuscations (X-OBF)

In this evaluation, the source pool is the non-obfuscated functions, and the pools of the three obfuscation types were used as the target pools. As shown in Table 5, there are three searching tasks: “SUB,” “FLA,” and “BCF,” which stand for “Ollvm-none vs. Ollvm-sub,” “Ollvm-none vs. Ollvm-fla,” and “Ollvm-none vs. Ollvm-bcf.” UniASM achieved average MRR and Recall@1 values of 83% and 77%, outperforming its closest baseline competitor by 15% and 22%.

Table 5: Performance on cross-obfuscation (X-OBF)

| | MRR (Ollvm) | | | | Recall@1 (Ollvm) | | | |
|----------|-------------|------------|------------|------------|------------------|------------|------------|------------|
| | SUB | FLA | BCF | Avg. | SUB | FLA | BCF | Avg. |
| Asm2vec | .74 | .42 | .21 | .46 | .66 | .34 | .19 | .40 |
| SAFE | .85 | .45 | .39 | .56 | .78 | .38 | .34 | .50 |
| PalmTree | .72 | .29 | .21 | .41 | .63 | .24 | .18 | .35 |
| jTrans | .88 | .69 | .58 | .72 | .81 | .58 | .49 | .63 |
| UniASM | .97 | .87 | .69 | .83 | .89 | .81 | .61 | .77 |

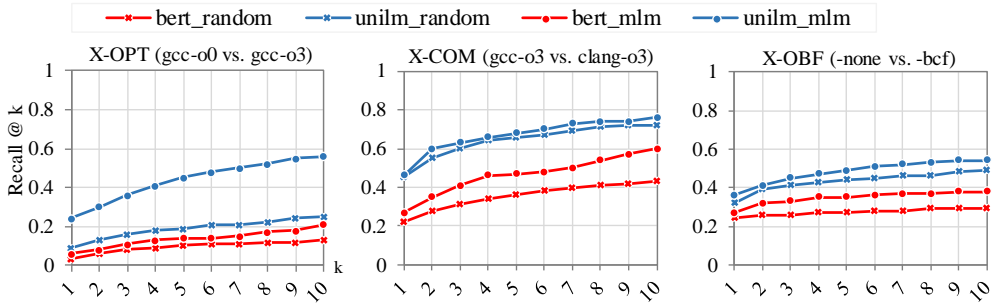
5.2 Ablation studies

In the ablation studies, we try to find the factors that affect the performance of binary embedding. We evaluated the performance of different backbone models (Section 5.2.1), training tasks (Section 5.2.2), and training corpora (Section 5.2.3) on three BCSO tasks: X-OPT, X-COM, and X-OBF. In addition, we compared the embedding space layout of different models (Section 5.2.4).

We use the Recall@k metric to evaluate the performance of the model. To ensure the fairness of the experiments, all the models have the same hyperparameters (Section 4.4) and use the same training and evaluation datasets (Section 4.1).

5.2.1 Backbone models

UniASM is based on the UniLM model, and the BERT model is used as a competitor of the backbone model. First, we evaluated BERT and UniLM with the initial random parameters (“bert_random” and “unilm_random” in Figure 5). Then, we trained the two models with an MLM task and compared the performance (“bert_mlm” and “unilm_mlm” in Figure 5). The MLM task is BERT’s default training task, which masks 15% of all tokens in each sequence at random.

**Figure 5:** Performance of different models

The results show that UniLM performs much better than BERT in all the BCSO tasks. The average Recall@k of UniLM improved by 78% over BERT when using random parameters. The improvement expanded to 105% when both were trained with the MLM task.

5.2.2 Training tasks

In this study, we first trained UniASM with one training task at a time, resulting in three pre-trained models: MLM, ALG, and SFP. In addition, we evaluated the combinations of the training tasks, resulting in another two pre-trained models: MLM+SFP and ALG+SPF.

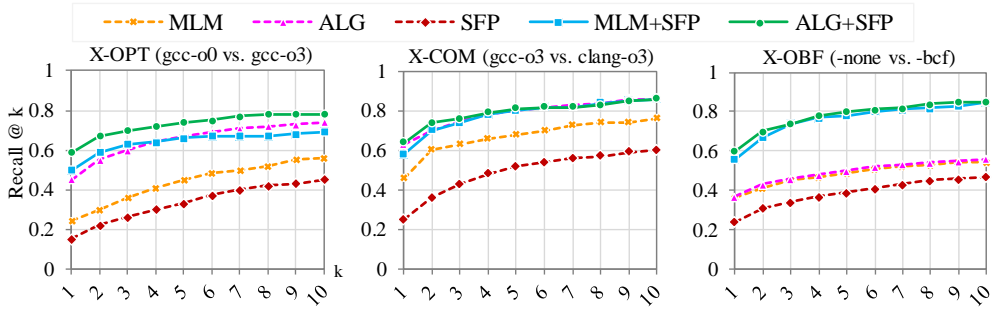


Figure 6: Performance of different training tasks

As shown in Figure 6, the model with ALG+SFP tasks outperforms all other competitors. When looking closely at the resulting data, we find some interesting details:

- One is that the ALG task shows high performance in both X-OPT and X-COM. However, the performance in X-OBF is relatively poor. As shown in Figure 6, the ALG task improves performance over MLM by an average of 53% in X-OPT and 18% in X-COM, but only 3% in X-OBF.
- Another is that the SFP task performs poorly in all BCSD tasks. However, it can significantly improve the model’s performance when combined with MLM or ALG. For the X-OBF task, SFP improves the average Recall@k of MLM from 0.48 to 0.76 and the average Recall@k of ALG from 0.49 to 0.78.

5.2.3 Training corpora

The training dataset is an important factor impacting the performance of the model. In this study, we prepared five different training datasets:

- **Default:** The assembly function in the training dataset was compiled with the no-inlining option “*-fno-inline,*” and the function was serialized in linear order (the address order). When tokenizing the assembly code, UniASM normalizes the instruction and treats the entire instruction as a token.
- **Inlining compilation:** Inlining is the default feature of the compiler, which eliminates call-linkage overhead and can expose other optimization opportunities. The source code was re-compiled without the option “*-fno-inline.*” The new dataset has 32% fewer functions than the default dataset because some functions are inlined into another function.
- **Random-walk:** The random-walk chooses a random path on the CFG of a function, which can extract structure information of the function. All of the functions in this dataset were serialized by random walks on the CFG.
- **Longest-walk:** The longest-walk is an optimized version of the random-walk, which choose the longest path on the CFG of a function. A longer path contains more semantic information about a function.
- **Small-token:** The small-token tokenization is more fine-grained than the default tokenization. Each word in the instruction was treated as a token instead of the whole instruction. For example, the instruction “`mov rax, [rbx+0x10]`” can be tokenized into four tokens: “`mov,`” “`rax,`” “`rbx,`” and “`0x10.`”

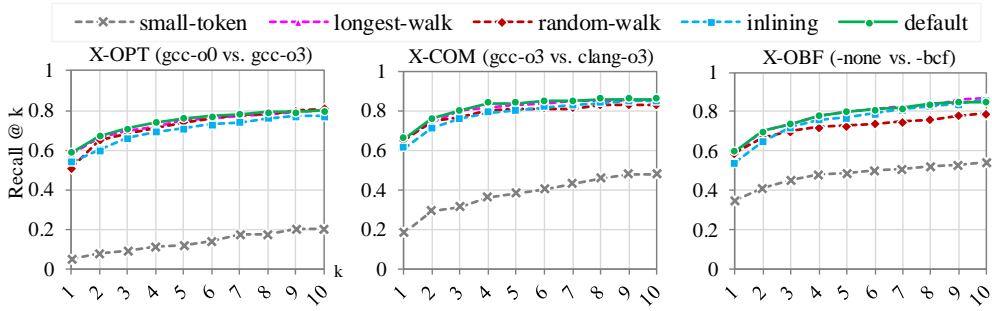


Figure 7: Performance of different training corpora

As shown in Figure 7, the dataset of small-token performs significantly worse than other datasets in all BCSO tasks, while the rest datasets achieve essentially the same performance. Surprisingly, the path-based datasets (random-walk and longest-walk) did not outperform the default linear dataset. We also find that the inlining dataset is slightly worse than the default dataset. The possible reason is that function inlining reduces the similarity of the function pairs, which makes the training more difficult.

5.2.4 Embedding space analysis

The function embeddings were all generated from the same evaluation dataset described in Section 4.1.2. We compared BERT and UniASM with different training tasks. “-random” means that the model uses the initial random parameters. We leverage t-SNE [40] to visualize the high-dimensional vectors. Each color indicates one compilation environment.

When calculating similarity, we want similar embeddings to be as close as possible and different embeddings as far as possible. As all functions of a compilation environment (the points in the same color) are considered different, a good embedding space should make the points uniformly distributed.

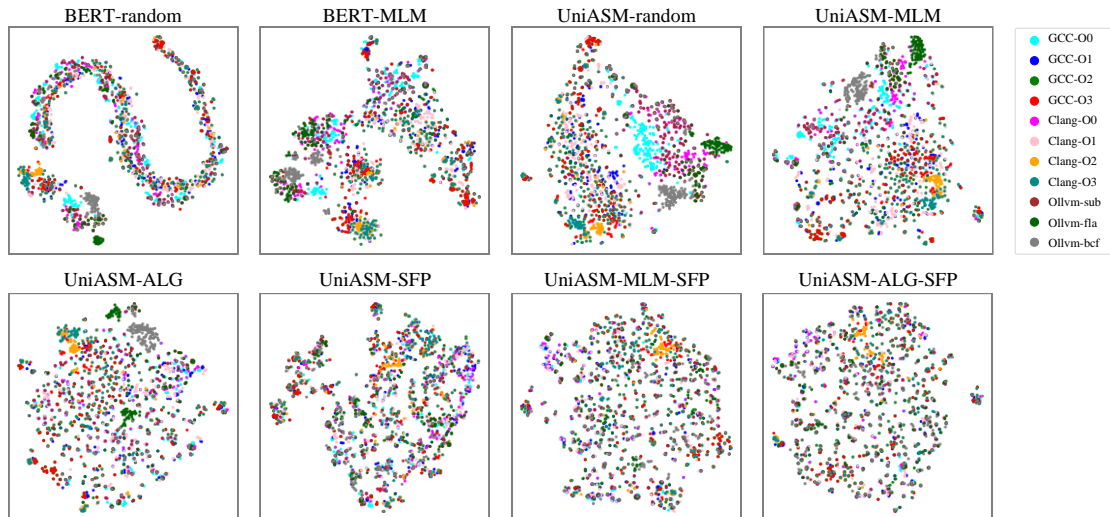


Figure 8: Embedding space of different models

As shown in Figure 8, the embeddings of UniASM are more uniformly distributed than BERT, which explains why UniASM performs better than BERT. When trained UniASM with different tasks, the embedding spaces significantly differ. The MLM and SFP did not distinguish the embeddings very well. The ALG did better, but there are still some local clusters.

The joint task ALG+SFP makes most of the embeddings uniformly distributed. The results of this study are very consistent with the previous ablation studies (Section 5.2.1 and Section 5.2.2).

5.3 Vulnerability searching

To evaluate UniASM’s performance on the real-world vulnerability search task, we randomly selected eight vulnerabilities from a known vulnerabilities dataset [39] as the search targets. Then we collected the affected software and compiled them by two compilers (GCC-7.5, Clang-10) with four optimization levels (O0, O1, O2, O3) and the obfuscator (Ollvm14) with three obfuscation types (*-sub*, *-fla*, *-bcf*). As a result, each software was compiled into 11 variants. For each vulnerability query, the source function pool is the 11 variants of the vulnerable function, and the target function pool is all of the functions in all the variants. The size of the target function pool for each project varies from 4,296 to 96,836. For example, the target function pool of CVE-2013-1944 from the curl-7.29.0 project contains 8334 functions.

As the source pool contains 11 vulnerable functions, we query each function in the target function pool and collect the top-11 results. The Recall@11 was used as the evaluation metric, meaning the model retrieves how many variants of vulnerable function in the top-11 results. We calculate the mean Recall@11 for all 11 queries. As shown in Table 6, UniASM outperforms all the baseline models, and its score is 29% to 207% higher than the leading baseline.

Table 6: Performance on vulnerability searching

| CVEs | Software | Pool | Models (Mean Recall@11) | | | | |
|---------------|----------------|-------|-------------------------|------|----------|--------|------------|
| | | | Asm2vec | SAFE | PalmTree | jTrans | UniASM |
| CVE-2013-1944 | curl-7.29.0 | 8334 | .16 | .27 | .14 | .27 | .77 |
| CVE-2015-8877 | libgd-2.1.1 | 4296 | .33 | .36 | .22 | .36 | .69 |
| CVE-2016-1541 | libarchive-3.1 | 15125 | .25 | .22 | .22 | .28 | .86 |
| CVE-2016-7163 | openjpeg-2.1 | 4804 | .17 | .38 | .26 | .24 | .45 |
| CVE-2016-8858 | openssh-7.3 | 53454 | .12 | .21 | .16 | .23 | .42 |
| CVE-2017-9051 | libav-12 | 23048 | .21 | .21 | .20 | .38 | .54 |
| CVE-2017-7866 | ffmpeg-2.8.6 | 96836 | .21 | .36 | .36 | .28 | .52 |
| CVE-2018-8970 | libressl-2.7.0 | 50762 | .21 | .27 | .21 | .18 | .35 |

6 Limitations

Cross-Architecture As the training dataset of UniASM consists of x86_64 code. Our pre-trained model can only be used for x86_64 binaries. However, UniASM is not limited to this and can be re-trained with the dataset of other architectures (e.g., ARM, MIPS, etc.).

Control flow semantics UniASM performs linear serialization of functions, so the current model cannot learn the control flow semantics. Although, our ablation studies show that the linear one is similar to the random-walk or the longest-walk. Existing work, such as jTrans, shows that control flow information is an important semantic component of functions. A reasonable representation of the control flow should be helpful and deserves further study.

Out-of-vocabulary Our tokenizer treats the whole instruction as a token, which makes the token contain more semantics information. However, a more complex token means a larger dictionary, leading to the OOV problem. In this paper, UniASM tries to mitigate the OOV problem by normalizing the instructions.

7 Conclusion and Future Work

In this paper, we propose UniASM, the first attempt to apply a UniLM-based model with two training tasks for BCSD. UniASM learns the semantics of assembly code and generates the function embeddings. The generated vectors can be used directly for similarity comparisons without fine-tuning. Experimental results show that UniASM has better performance than the top-performing baselines. In addition, we designed ablation studies to explore the impact factors on the model’s accuracy in BCSD tasks.

The ALG task gives the model the ability to generate assembly code. In the future, we plan to apply this ability to more valuable downstream tasks, such as code transformation, automatic coding, etc.

References

- [1] Bingchang Liu, Wei Huo, Chao Zhang, Wenchao Li, Feng Li, Aihua Piao, and Wei Zou. `adiff`: Cross-version binary code similarity detection with dnn. In Proceedings of the 33rd ACM/IEEE International Conference on Automated Software Engineering, ASE 2018, Montpellier, France, September 3-7, 2018, pages 667–678.
- [2] Fei Zuo, Xiaopeng Li, Zhixin Zhang, Patrick Young, Lannan Luo, and Qiang Zeng. Neural machine translation inspired binary code similarity comparison beyond function pairs. In 26th Annual Network and Distributed System Security Symposium, NDSS 2019, San Diego, California, USA, February 24-27, 2019.
- [3] Silvio Cesare and Yang Xiang. Malware variant detection using similarity search over sets of control flow graphs. In IEEE 10th International Conference on Trust, Security and Privacy in Computing and Communications, TrustCom 2011, Changsha, China, 16-18 November, 2011, pages 181–189.
- [4] Silvio Cesare, Yang Xiang, and Wanlei Zhou. Control flow-based malware variant detection. IEEE Transactions on Dependable and Secure Computing, 11:307–317, 2014.
- [5] Csongor Tamás, Dorottya Papp, and Levente Buttyán. Simbiota: Similarity-based malware detection on IoT devices. In Proceedings of the 6th International Conference on Internet of Things, Big Data and Security, IoTBDS 2021, Online Streaming, April 23-25, 2021, pages 58–69.
- [6] Yikun Hu, Yuanyuan Zhang, Juanru Li, and Dawu Gu. Binary code clone detection across architectures and compiling configurations. In Proceedings of the 25th International Conference on Program Comprehension, ICPC 2017, Buenos Aires, Argentina, May 22-23, 2017, pages 88–98.
- [7] Steven H. H. Ding, Benjamin C. M. Fung, and Philippe Charland. Kam1n0: Mapreduce-based assembly clone search for reverse engineering. In Proceedings of the 22nd ACM SIGKDD International Conference on Knowledge Discovery and Data Mining, San Francisco, CA, USA, August 13-17, 2016, pages 461–470.
- [8] Zhengzi Xu, Bihuan Chen, Mahinthan Chandramohan, Yang Liu, and Fu Song. Spain: Security patch analysis for binaries towards understanding the pain and pills. In Proceedings of the 39th International Conference on Software Engineering, ICSE 2017, Buenos Aires, Argentina, May 20-28, 2017, pages 462–472.
- [9] Andreas Sæbjørnsen, Jeremiah Willcock, Thomas Panas, Daniel J. Quinlan, and Zhendong Su. Detecting code clones in binary executables. In Proceedings of the Eighteenth International Symposium on Software Testing and Analysis, ISSTA 2009, Chicago, IL, USA, July 19-23, 2009, pages 117–128.

- [10] Yuede Ji, Lei Cui, and H. Howie Huang. Buggraph: Differentiating source-binary code similarity with graph triplet-loss network. In ASIA CCS '21: ACM Asia Conference on Computer and Communications Security, Virtual Event, Hong Kong, June 7-11, 2021, pages 702–715.
- [11] Xiaojun Xu, Chang Liu, Qian Feng, Heng Yin, Le Song, and Dawn Xiaodong Song. Neural network-based graph embedding for crossplatform binary code similarity detection. In Proceedings of the 2017 ACM SIGSAC Conference on Computer and Communications Security, CCS 2017, Dallas, TX, USA, October 30 - November 03, 2017, pages 363–376.
- [12] Steven H. H. Ding, Benjamin C. M. Fung, and Philippe Charland. Asm2vec: Boosting static representation robustness for binary clone search against code obfuscation and compiler optimization. In 2019 IEEE Symposium on Security and Privacy, SP 2019, San Francisco, CA, USA, May 19-23, 2019, pages 472–489.
- [13] Quoc V. Le and Tomas Mikolov. Distributed representations of sentences and documents. In Proceedings of the 31th International Conference on Machine Learning, ICML 2014, Beijing, China, 21-26 June 2014, volume 32 of JMLR Workshop and Conference Proceedings, pages 1188–1196.
- [14] Luca Massarelli, Giuseppe Antonio Di Luna, Fabio Petroni, Leonardo Querzoni, and Roberto Baldoni. Safe: Self-attentive function embeddings for binary similarity. In Detection of Intrusions and Malware, and Vulnerability Assessment - 16th International Conference, DIMVA 2019, Gothenburg, Sweden, June 19-20, 2019, Proceedings, volume 11543 of Lecture Notes in Computer Science, pages 309–329.
- [15] TensorFlow. Word2vec skip-gram implementation in tensorflow. <https://tensorflow.google.cn/tutorials/text/word2vec>, 2022.
- [16] Zhouhan Lin, Minwei Feng, Cícero Nogueira dos Santos, Mo Yu, Bing Xiang, Bowen Zhou, and Yoshua Bengio. A structured self-attentive sentence embedding. In 5th International Conference on Learning Representations, ICLR 2017, Toulon, France, April 24-26, 2017, Conference Track Proceedings.
- [17] Xuezixiang Li, Qu Yu, and Heng Yin. Palmtree: Learning an assembly language model for instruction embedding. In CCS '21: 2021 ACM SIGSAC Conference on Computer and Communications Security, Virtual Event, Republic of Korea, November 15 - 19, 2021, pages 3236–3251.
- [18] Jacob Devlin, Ming-Wei Chang, Kenton Lee, and Kristina Toutanova. BERT: Pre-training of deep bidirectional transformers for language understanding. In proceedings of the 2019 Conference of the North American Chapter of the Association for Computational Linguistics: Human Language Technologies, NAACL-HLT 2019, Minneapolis, MN, USA, June 2-7, 2019, Volume 1, pages 4171–4186.
- [19] Hao Wang, Wenjie Qu, Gilad Katz, Wenyu Zhu, Zeyu Gao, Hang Qiu, Jianwei Zhuge, and Chao Zhang. jtrans: jump-aware transformer for binary code similarity detection. In ISSTA '22: 31st ACM SIGSOFT International Symposium on Software Testing and Analysis, Virtual Event, South Korea, July 18 - 22, 2022, pages 1–13.
- [20] Hex-rays. IDA FLIRT. <https://hex-rays.com/products/ida/tech/flirt/>, 2022.
- [21] Emily R. Jacobson, Nathan E. Rosenblum, and Barton P. Miller. Labeling library functions in stripped binaries. In Proceedings of the 10th ACM SIGPLAN-SIGSOFT workshop on Program analysis for software tools, PASTE'11, Szeged, Hungary, September 5-9, 2011, pages 1–8.

- [22] Sebastian Eschweiler, Khaled Yakdan, and Elmar Gerhards-Padilla. discover: Efficient cross-architecture identification of bugs in binary code. In 23rd Annual Network and Distributed System Security Symposium, NDSS 2016, San Diego, California, USA, February 21-24, 2016.
- [23] Thomas Dullien and Rolf Rolles. Graph-based comparison of executable objects (english version). In SSTIC, volume 5, page 3, 2005.
- [24] Qian Feng, Rundong Zhou, Chengcheng Xu, Yao Cheng, Brian Testa, and Heng Yin. Scalable graph-based bug search for firmware images. In Proceedings of the 2016 ACM SIGSAC Conference on Computer and Communications Security, Vienna, Austria, October 24-28, 2016, pages 480–491.
- [25] Jannik Pewny, Behrad Garmany, Robert Gawlik, Christian Rossow, and Thorsten Holz. Cross-architecture bug search in binary executables. *Information Technology*, 59:83–91, 2015.
- [26] Mahinthan Chandramohan, Yinxing Xue, Zhengzi Xu, Yang Liu, Chia Yuan Cho, and Hee Beng Kuan Tan. Bingo: cross-architecture cross-os binary search. In Proceedings of the 24th ACM SIGSOFT International Symposium on Foundations of Software Engineering, FSE 2016, Seattle, WA, USA, November 13-18, 2016, pages 678–689.
- [27] Shuai Wang and Dinghao Wu. In-memory fuzzing for binary code similarity analysis. In Proceedings of the 32nd IEEE/ACM International Conference on Automated Software Engineering, ASE 2017, Urbana, IL, USA, October 30 - November 03, 2017, pages 319–330.
- [28] Zeping Yu, Rui Cao, Qiyi Tang, Sen Nie, Junzhou Huang, and Shi Wu. Order matters: Semantic-aware neural networks for binary code similarity detection. In The Thirty-Fourth AAAI Conference on Artificial Intelligence, AAAI 2020, The Thirty-Second Innovative Applications of Artificial Intelligence Conference, IAAI 2020, The Tenth AAAI Symposium on Educational Advances in Artificial Intelligence, EAAI 2020, New York, NY, USA, February 7-12, 2020, pages 1145–1152.
- [29] Jianlin Su. Simbert: Integrating retrieval and generation into BERT. <https://github.com/ZhuiyiTechnology/simbert>, 2022.
- [30] Li Dong, Nan Yang, Wenhui Wang, Furu Wei, Xiaodong Liu, Yu Wang, Jianfeng Gao, M. Zhou, and Hsiao-Wuen Hon. Unified language model pre-training for natural language understanding and generation. In Advances in Neural Information Processing Systems 32: Annual Conference on Neural Information Processing Systems 2019, NeurIPS 2019, December 8-14, 2019, Vancouver, BC, Canada, pages 13042–13054.
- [31] Pascal Junod, Julien Rinaldini, Johan Wehrli, and Julie Michielin. Obfuscator-llvm – software protection for the masses. In 1st IEEE/ACM International Workshop on Software Protection, SPRO 2015, Florence, Italy, May 19, 2015, pages 3–9.
- [32] heroims. Obfuscator-llvm. <https://github.com/heroims/obfuscator,2022>.
- [33] RadareOrg. radare2. <https://github.com/radareorg/radare2, 2022>.
- [34] oalieno. Unofficial implementation of asm2vec using pytorch. <https://github.com/oalieno/asm2vec-pytorch, 2022>.
- [35] SAFE Team. Official implementation of safe. <https://github.com/gadiluna/SAFE, 2022>.
- [36] PalmTree Team. Official implementation of palmtree. <https://github.com/palmtree/PalmTree, 2022>.
- [37] jTrans Team. Official implementation of jtrans. <https://github.com/vul337/jTrans, 2022>.
- [38] Hex-rays. Ida pro disassembler and debugger. <https://www.hexrays.com/products/ida/index.shtml, 2022>.
- [39] SecretPatch. Vulnerabilities dataset. <https://github.com/SecretPatch/Dataset, 2022>

- [40] Laurens van der Maaten and Geoffrey Hinton. Visualizing data using t-SNE. *Journal of Machine Learning Research*, 9:2579–2605, 2008.